Safety in Extreme Environments (2022) 4:35–45
https://doi.org/10.1007/s42797-022-00050-8

RESEARCH ARTICLE

Adsorption, electrochemical and theoretical studies on the protective effect of N-(5-bromo-2-hydroxybenzylidene) isonicotinohydrazide on carbon steel corrosion in aggressive acid environment

Augustine A. Chokor[1] · Cordelia U. Dueke-Eze[2] · Lebe A. Nnanna[3] · Nkem B. Iroha[1]

Received: 26 November 2021 / Revised: 4 January 2022 / Accepted: 4 January 2022 / Published online: 26 January 2022

Abstract

A new Schiff base, N-(5-bromo-2-hydroxybenzylidene) isonicotinohydrazide (NBHI), has been synthesized and studied as an inhibitor of X70 carbon steel (CS) corrosion in aggressive 1 M HCl environment using gravimetric, electrochemical impedance spectroscopy (EIS) tests, potentiodynamic polarization (PDP) and scanning electron microscopy (SEM). The inhibition efficiency was found to increase with increase in NBHI concentration but decreased with rise in temperature. Inhibition efficiencies up to 96.7%, 97.0% and 94.2% were obtained respectively for weight loss, EIS and polarization measurements at 1.00 mM and 303 K. Polarization studies indicate that NBHI essentially behaved as a mixed-type inhibitor controlling both anodic and cathodic reactions. EIS results indicated that charge transfer resistance (R_{ct}) increased while double layer capacitance (C_{dl}) decreased with increasing NBHI concentration. The adsorption of NBHI onto the X70 CS surface obeyed Langmuir adsorption isotherm. SEM analysis supported the protective film formation of NBHI on the steel surface. Quantum chemical calculations were used to study NBHI reactivity and the results complimented well with the experimental data.

Keywords Schiff base · X70 carbon steel · Corrosion inhibition · EIS · Quantum chemical calculation · Mixed-type inhibitor

Introduction

Corrosion is a huge challenge in the petroleum industry, affecting seriously the entire production process and eventually leads to tremendous economic losses and structural failure (Finšgar and Jackson 2014). X70 steel is one of the API recommended steel grade in the petroleum industry due to its known superiority in resisting corrosion when compared with other steel alloys. During well acidization to improve oil recovery, 1 M HCl solution is usually used and this process over the years has proven to deteriorate the steel. To minimize the damage caused by this aggressive solution, corrosion inhibitors are usually introduced in the acid treatment solution (El Kacimi et al. 2020; Iroha and Nnanna 2021). These inhibitors get adsorbed on the steel surface, either by physisorption or chemisorption through the π electrons of the aromatic rings, heteroatoms like O, N, P and S, or conjugate double bonds. The inhibitors hinders or reduces the rate dissolution by blocking the active sites (Zeino et al. 2018; Iroha et al. 2005; Belfilali et al. 2012; Iroha and James 2018). However, majority of inorganic/organic corrosion inhibitors already in use mostly those containing phosphates and heavy metals are toxic and not environmental friendly. The increasing need for anticorrosion agents that are eco-friendly have necessitated the development of corrosion inhibitors that are not only efficient but also free of organic phosphates and heavy metals (Ramaganthan et al. 2015; Iroha and Akaranta 2020).

Some of the eco-friendly anticorrosion agents used as steel corrosion inhibitors includes plant extracts (Umoren 2016; Boumhara et al. 2014), Polymers (Abdallah et al. 2020) and pharmaceutical compounds (Iroha and Nnanna 2021). These inhibitors have shown excellent corrosion inhibition on different types of steel. Corrosion inhibition was

✉ Nkem B. Iroha
irohanb@fuotuoke.edu.ng

[1] Department of Chemistry, Federal University Otuoke, P.M.B 126, Yenagoa, Bayelsa State, Nigeria

[2] Chemistry Department, University of Lagos, Akoka, Lagos State, Nigeria

[3] Department of Physics, Michael Okpara University of Agriculture Umudike, Abia State, Umudike, Nigeria

seen to varry generally with immersion time, temperature and concentration of inhibitor. Recently, several corrosion researchers have studied the performance of synthesized Schiff bases in inhibiting steel corrosion in acidic environments (Khaled et al. 2010; Okey et al. 2020; Iroha et al. 2021). These Schiff bases have exhibited high inhibition performance for steel corrosion in both H_2SO_4 (Farag and Hegazy 2013) and HCl (Ansari et al. 2014; Hegazy et al. 2012) solutions. Some hydrazide derivatives have be studied as inhibitors for the corrosion of various metals and in different acid media (Mohan et al. 2013; Iroha and Dueke-Eze 2021; Chakravarthy and Mohana 2013). Hydrazide derivatives which are a type of organic compounds containing a N-N covalent bond having at least one acyl group substituent, have gained popularity due to their antioxidant, antibacterial, anticancer, analgesic, antimalarial, antiplatelet and anti-inflammatory activity (Narang et al. 2012; Sainia et al. 2014). More so, they have been employed as efficient corrosion inhibitors for various metals. The π-bond, planar structure and electron lone pairs on the nitrogen atom makes hydrazide-based Schiff base inhibitors to adsorb easily on metal surfaces forming a dative-covalent bond with the metals.

The main objective of this study is to elucidate a new Schiff base, N-(5-bromo-2-hydroxybenzylidene) isonicotinohydrazide (NBHI) as corrosion inhibitor for X70 steel in 1 M HCl solution. We selected this compound because it can be conveniently synthesized from less expensive chemicals that are commercially available. The inhibitor is a non-toxic, water-soluble, biodegradable and good adsorbent on steel surfaces. Gravimetric and electrochemical (PDP and EIS) measurements were utilized in monitoring the corrosion process; SEM was utilized for surface morphological investigations. Computational analysis with the use of density functional theory (DFT) enabled inhibitor-metal interactions assessment for the NBHI inhibitor.

Experimental

Inhibitor synthesis

The studied NBHI inhibitor was synthesized as earlier reported by Dueke-Eze et al. (2020). The chemical equation for the synthesis is shown in Fig. 1.

Materials

The aggressive solution used in this study, 1 M HCl, was made by diluting 37% HCl analar grade with distilled water. The X70 steel specimens utilized for gravimetric and electrochemical studies contains (in wt%); C: 0.23; P: 0.03; Mn: 1.10; S: 0.008; Ti: 0.005; Ni: 0.35; Cu: 0.15; Pb: 0.002; Nb: 0.012; and balance iron. The specimens were prepared by first abrading with emery paper (grades 400-1200), afterwards washed with double-distilled water and then acetone, dried and weighed. The steel coupons cut in dimensions of 2.0 cm × 2.0 cm × 0.1 cm were utilized for the gravimetric measurement. For electrochemical measurement, X70 steel specimens with dimensions 1.5 cm × 1.5 cm × 0.1 cm, used as the working electrode were embedded into epoxy resin with 0.85 cm^2 exposed area to the electrolyte. The concentrations of the new Schiff base, NBHI ranged from 0.25 mM to 1.00 mM.

Gravimetric analysis

The gravimetric (weight loss) tests were conducted using ASTM G31-72 standard (ASTM 2004) in bare and inhibited 1 M HCl solution at different NBHI concentrations. The pre-weighed X70 steel specimens were immersed in the varying solutions for 7 h at 30, 40 and 50 °C unstirred. The immersed steel samples were removed after the expiry time, washed thoroughly with bidistilled water and ethanol, dried with acetone and re-weighed. The weight loss (ΔW) was deduced from the difference in weight of X70 steel specimens before and after submersion in the various test solutions. Triplicate tests were conducted to ensure the experiment is reproducible, and the average of the three values reported. The corrosion rates (C_R) were calculated from the weight loss data as expressed:

$$C_R = \frac{\triangle W}{At} \tag{1}$$

where A represents area and t is the time of exposure of the X70 steel specimens. The inhibition efficiency ($\eta_{WL}\%$) of NBHI was computed as follows:

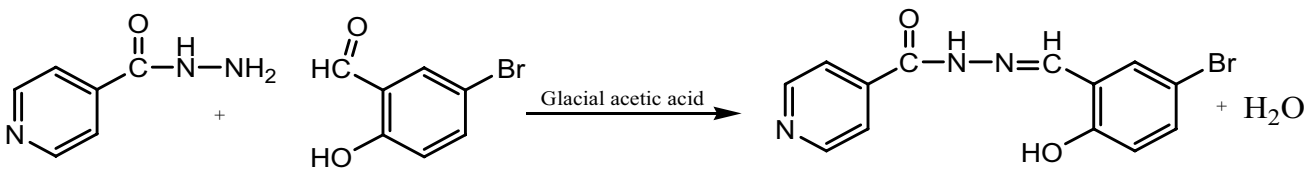

Fig. 1 Chemical equation for NBHI synthesis

$$n_{WL}\% = \frac{C_{R(b)} - C_{R(i)}}{C_{R(b)}} \times 100 \quad (2)$$

where $C_{R(b)}$ and $C_{R(i)}$ are the corrosion rates of X70 steel in bare and inhibited1 M HCl solution, respectively.

Electrochemical measurement

Electrochemical tests were performed using a G-300 Gamry Potentiostat/Galvanostat at 30 °C, in an assembly of three electrode cell. The X70 steel was the working electrode (WE), saturated calomel electrode (SCE) used as reference electrode and platinum used as counter electrode. The data were analyzed using Echem Analyst 5.0 software package. The WE was submerged for 30 min, in the test solution at open-circuit potential (OCP) for stability before measurement. EIS measurements were conducted at OCP over the frequency range of 1000 Hz–10 Hz with signal amplitude of 10 mA. PDP measurements were carried out in the potential range of ±250 mV from E_{corr} at a scan rate of 0.1 mV/s. All tests were run three times to ensure data reproducibility.

SEM analysis

Surface morphological examinations of the X70 steel were performed by SEM model ZEISS EVO. SEM micrographs of the X70 steel surface were obtained after immersion in bare 1 M HCl and in presence of 1.00 mM NBHI inhibitor for 7 h at 30 °C. The specimens were retrieved after immersion, washed thoroughly with distilled water and dried with acetone before taking SEM pictures.

Quantum chemical analysis

The quantum chemical computation carried out with the Spartan 14.0 software was performed through DFT using the B3LYP level with 6-311G (d, p) basis sets. The obtained values of energy of the highest occupied molecular orbital (E_{HOMO}) and energy of lowest unoccupied molecular orbital (E_{LUMO}) were used to compute energy gap (ΔE), electronegativity (χ), global hardness (η), global softness (σ) and fraction of electron transferred (ΔN) as expressed in the following equations (Arivazhagan and Subhasini 2012; Maduelosi and Iroha 2021):

$$\Delta E = E_{LUMO} - E_{HOMO} \quad (3)$$

$$\chi = -\frac{1}{2}\left(E_{LUMO} + E_{HOMO}\right) \quad (4)$$

$$\eta = \frac{1}{2}\left(E_{LUMO} - E_{HOMO}\right) \quad (5)$$

$$\sigma = \frac{1}{\eta} \quad (6)$$

$$\Delta N = \frac{\chi_{Fe} - \chi_{inh}}{2(\eta_{Fe} + \eta_{inh})} \quad (7)$$

where $\chi_{Fe} = 7.0$ eV and $\eta_{Fe} = 0$ for bulk Fe.

Result and discussion

Gravimetric measurement

Influence of concentration

Table 1 shows the C_R and η_{WL} in blank 1 M HCl and in various concentrations of NBHI and at various temperatures. The data clearly reveal that the C_R decreased and the $\eta_{WL}\%$ increased upon addition of NBHI. As the concentration of NBHI increases, a continuous decease and increase in C_R and η_{WL} respectively was observed. The η_{WL} reached a maximum of 96.7% at 30 °C and 1.00 mM concentration of NBHI indicating that the new synthesized Schiff base performed well as a corrosion inhibitor for X70 steel. The corrosion inhibition is possibly due to the adsorption of NBHI molecule at the steel/$HCl_{(aq)}$ interface (Lebrini et al. 2008; Madueke and Iroha 2018).

Table 1 The C_R and η_{WL} computed from gravimetric measurements of X70 in 1 M HCl consisting different concentrations of NBHI at various temperatures

Temperature (°C)	Concentration (mM)	C_R (mg cm^{-2} h^{-1})	η_{WL} (%)
30 °C	Blank	2.764	–
	0.25	1.006	63.6
	0.50	0.682	75.3
	0.75	0.251	90.9
	1.00	0.090	96.7
40 °C	Blank	5.168	–
	0.25	2.072	59.9
	0.50	1.385	73.3
	0.75	0.594	88.5
	1.00	0.297	94.3
50 °C	Blank	7.905	–
	0.25	3.586	54.6
	0.50	2.175	72.5
	0.75	1.314	83.4
	1.00	0.984	87.6
60 °C	Blank	9.714	–
	0.25	4.681	51.8
	0.50	3.097	68.1
	0.75	1.998	79.4
	1.00	1.285	86.8

Effect of temperature

The influence of temperature on C_R and η_{WL} for X70 steel in bare 1 M HCl and inhibited with NBHI was studied in the range of temperature 30-60 °C. Table 1 reveals that the C_R increased both in bare and inhibited solutions by increasing the system temperature. On the other hand, the η_{WL} decreased with temperature rise. This suggest that while inhibition occurs due to inhibitors adsorption on the steel surface, an increase in temperature may have aided the desorption of the inhibitor. This desorption effect could be due to bonds between the steel surface and inhibitor which tends to release the inhibitor molecules back to the solution thereby exposing the steel to further dissolution. The temperature dependence on C_R is key in determining the activation parameters by using the Arrhenius equation given as:

$$\log C_R = \frac{-E_a}{2.303RT} + \log A \tag{8}$$

where A is the pre-exponential factor, E_a represents activation energy, R is the gas constant and T is the absolute temperature. A plot of log C_R versus 1/T produces straight lines as displayed in Fig. 2a. The slope of the straight lines is -E_a/2.303R, from where E_a values were computed and listed in Table 2. The data reveal that E_a values increase upon addition of NBHI to the 1 M HCl solution which suggest physisorption on the steel surface (James and Iroha 2019). An alternative form of Arrhenius equation known as Transition state equation (Ekanem et al. 2010) is given in Eq. 9, where h represents the Planck's constant, N is the Avogadro number, R and T retain their meanings, ΔS* is the activation entropy and ΔH* is the activation enthalpy.

Table 2 Activation parameters for X70 steel in 1 M HCl without and with different concentrations of NBHI

Conc (mM)	E_a (kJ/mol)	ΔH^* (kJ/mol)	ΔS^* (J/mol/K)
Blank	24.78	21.36	−168.32
0.25	27.81	24.89	−152.07
0.50	29.15	26.30	−150.25
0.75	30.90	27.95	−147.78
1.00	41.22	29.43	−146.03

$$\log \frac{C_R}{T} = \log\left(\frac{R}{Nh}\right) + \left(\frac{\Delta S^*}{2.303R}\right) - \left(\frac{\Delta H^*}{2.303RT}\right) \tag{9}$$

Plotting log (C_R/T) versus 1/T gives straight lines (Fig. 2b) with intercept log (R/Nh) + ($\Delta S^*/2.303R$) and slope $-\Delta H^*/2.303R$ from where values of ΔS^* and ΔH^* were computed and presented in Table 2. Close look at Table 2 reveal that ΔS^* values in the presence of NBHI are less negative than that in bare acid, indicating that the degree of disorderliness increases on going from the reactants to activated complex (Yadav et al. 2013; Iroha et al. 2020). The values of ΔH^* are positive reflecting the endothermic nature of X70 steel dissolution process.

Adsorption isotherm

The inhibitor adsorption caused by the interactions between the charged steel surface and the inhibitor molecules which

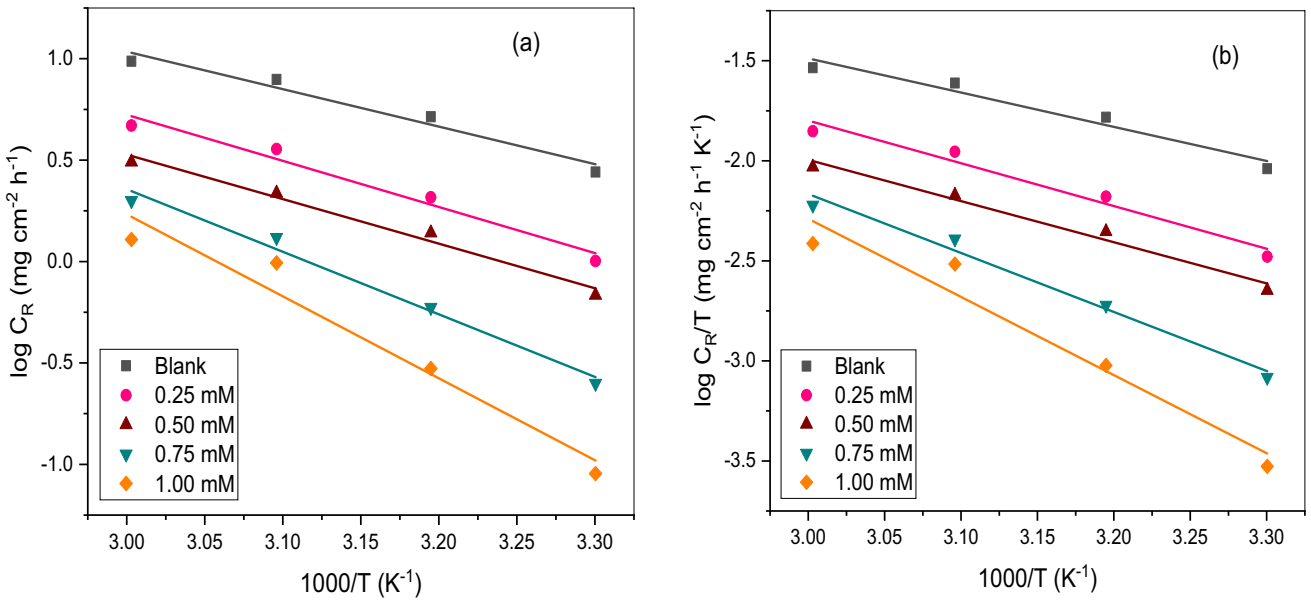

Fig. 2 Plots of **a** log C_R vs. 1/T and **b** log C_R/T vs. 1/T for X70 steel dissolution in 1 M HCl without and with various concentrations of NBHI

results to protective films formation on the steel surface is a surface phenomenon. Basic information relating to the nature of interaction between steel surfaces and inhibitor can be provided by the adsorption isotherm. The results obtained by fitting the surface coverage ($\theta = \eta_{WL}/100$) as a function of inhibitor concentration (C_{inh}) to various adsorption isotherms reveal that Langmuir isotherm gave the best fit according to Eq. 10:

$$\frac{C_{inh}}{\theta} = \frac{1}{K_{ads}} + C_{inh} \tag{10}$$

where K_{ads} is the adsorption equilibrium constant. Linear graphs obtained by plotting C_{inh}/θ versus C_{inh} (Fig. 3) and with regression (R^2) values close to unity suggest that the adsorption of NBHI on the X70 steel surface in 1 M HCl obeys the Langmuir isotherm (Noor and Al-Moubaraki 2008; Iroha and Hamilton-Amachree 2018). The slope values which are close to 1 suggest associative inhibitor adsorption at the steel surface (Hegazy et al. 2010). The K_{ads} values is computed from the intercept ($1/K_{ads}$) and listed in Table 3. The relatively high K_{ads} values are pointers to the high ability of NBHI to adsorb on the steel surface, which was found to diminish as the temperature increases (Madkour and Elroby 2015; Iroha et al. 2015). The adsorption free energy (ΔG^0_{ads}) is related to K_{ads} by the equation:

$$K_{ads} = \frac{1}{55.5}\exp\left(\frac{-\Delta G^0_{ads}}{RT}\right) \tag{11}$$

where 55.5 is concentration of water in solution (M), R and T retain their meanings. Computed ΔG^0_{ads} values are also listed in Table 3. Negative ΔG^0_{ads} values as revealed in Table 3 indicate the spontaneous process of NBHI adsorption on the X70 steel surface (Bentrah et al. 2014). It has been noted that

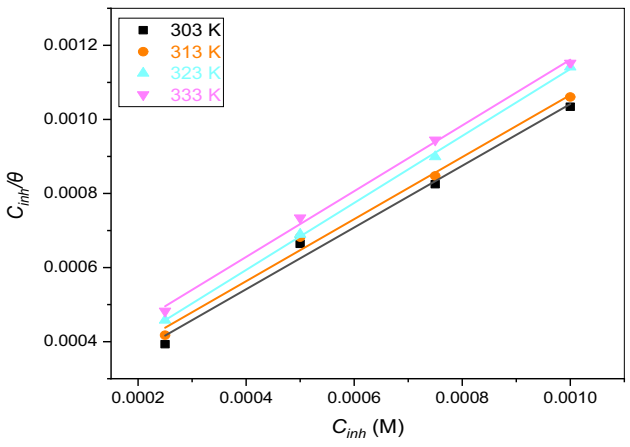

Fig. 3 Langmuir isotherm plot for NBHI on X70 steel in 1 M HCl various temperatures

Table 3 Langmuir adsorption isotherm parameters for NBHI deduced from gravimetric measurement at different temperatures

Temp. (K)	Intercept	Slope	R^2	K_{ads} (M^{-1})	ΔG^0_{ads} (kJ/mol)
303	2.08×10^{-4}	0.8337	0.9900	4807	−31.47
313	2.28×10^{-4}	0.8378	0.9921	4385	−32.27
323	2.32×10^{-4}	0.9043	0.9993	4310	−33.26
333	2.74×10^{-4}	0.8875	0.9973	3650	−33.83

ΔG^0_{ads} values within −20 kJ mol^{-1} or less negative relates to physisorption while more negative than −40 kJ mol^{-1} ΔG^0_{ads} values shows chemisorption (James and Iroha 2021). The report from our studies presents ΔG^0_{ads} values between −33.83 to −32.47 kJ mol^{-1}, indicating mixed-type (physical and chemical) adsorption mechanism (Messali et al. 2017).

Electrochemical impedance spectroscopy

EIS studies were carried out to reveal the mode of electrochemical process that take place at the steel/acid interface without and with addition of NBHI. Nyquist plots for X70 steel submerged in 1 M HCl solution without and in presence of different NBHI formulations are depicted in Fig. 4a. The Nyquist plots are generally regarded as a single depressed semicircle referred mostly to as frequency dispersion, resulting because of different physical phenomenon like heterogeneities, roughness, grain boundaries, impurities and surface active sites distribution (Chakravarthy and Mohana 2013) There was no change in the shape of the Nyquist plots for the various NBHI concentrations in 1 M HCl solution. However, the diameter of curves increases at higher inhibitor concentrations which is probably due to the inhibition of the X70 steel by NBHI. The inhibitor molecules block the active sites on the steel surface resulting to adsobed film formation, protecting the steel from the corrosive medium (Singh et al. 2015).

The equivalent circuit used in fitting the impedence curves consists of charge transfer resistance (R_{ct}), solution resistance (R_s) and constant phase element (CPE) as depicted in Fig. 4b. The CPE is used instead of capacitance for more precise fitting of the curves. The CPE impedance (Z_{CPE}) can be expressed by:

$$Z_{CPE} = \frac{(j\omega)^{-n}}{Y_0} \tag{12}$$

where ω is the angular frequency (i.e., $\omega = 2\pi f_{max}$); f_{max} is the frequency at which the imaginary component (Z_{im}) of the impedance is maximal. The EIS parameters deduced from the equivalent circuit are presented in Table 4. The values

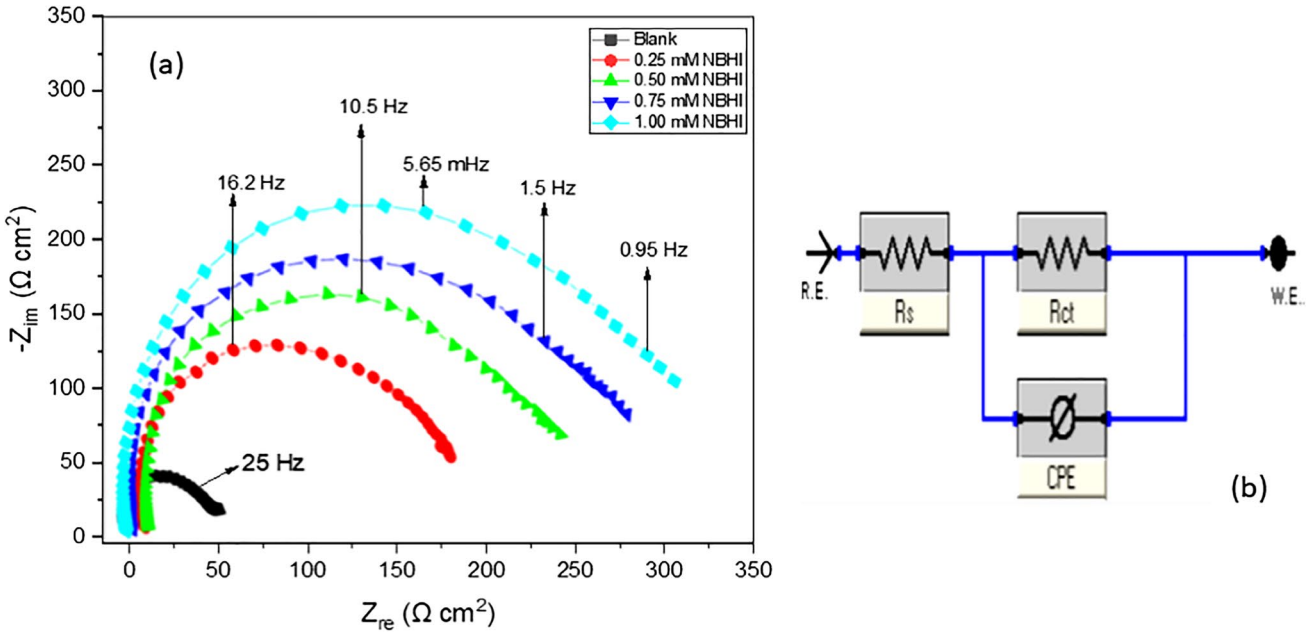

Fig. 4 **a** Nyquist plots for X70 steel in uninhibited 1 M HCl solutions and inhibited with various NBHI concentration **b** Equivalent circuit used in fitting the impedance plots

of double-layer capacitance (C_{dl}) was computed from the values of n (phase shift) and Y_0 (CPE constant), which are parameter of the CPE, according to the equation:

$$C_{dl} = Y_0(\omega_m)^{n-1} \tag{13}$$

where ω_m is the angular frequency at maximum Z_{im}. The inhibition efficiency (η_{EIS}) were computed utilizing the expression:

$$\eta_{EIS}(\%) = \frac{R'_{ct} - R_{ct}}{R'_{ct}} \times 100 \tag{14}$$

where R'_{ct} and R_{ct} are the charge transfer resistances for the inhibited and uninhibited solutions respectively. The results in Table 4 revealed an enhancement in R_{ct} values on increasing NBHI concentration while C_{dl} values were significantly brought down. The enhancement in the values of R_{ct} as NBHI concentration increases resulted to the increased diameter of the Nyquist plots semicircle, indicating that NBHI reduced X70 steel corrosion in 1 M HCl. The decrease in C_{dl} which mainly results from dielectric constant reduction and/or rise in double layer thickness indicates the protective effect of NBHI by its attachment on the steel surface.

Potentiodynamic polarization studies

Potentiodynamic polarization studies gives insight on how the inhibitor influences the cathodic and anodic corrosion reactions. A typical PDP plot for X70 steel corrosion in 1 M HCl without and in presence of NBHI is depicted in Fig. 5. The parameters deduced from the plot such as the corrosion current density (i_{corr}), the corrosion potential (E_{corr}), cathodic Tafel slopes (β_c), anodic Tafel slopes (β_a) and inhibition efficiency (η_{PDP} %) are listed in Table 5. The inhibition efficiency (η_{PDP} %) was computed using the expression:

Table 4 Impedance parameters for X70 steel corrosion in uninhibited 1 M HCl solutions and inhibited with various NBHI concentration at 303 K

Conc. (M)	R_s (Ω cm^2)	R_{ct} (Ω cm^2)	Q ($\mu\Omega^{-1}$ s^n cm^{-2})	C_{dl} (μF cm^{-2})	n	η_{EIS} (%)
Blank	0.84	12.6	194.5	137.9	0.891	–
0.25	0.81	38.1	169.0	82.5	0.904	66.9
0.50	1.19	53.5	132.6	51.8	0.908	76.4
0.75	1.03	70.4	109.3	26.4	0.912	82.1
1.00	1.21	86.8	89.5	10.1	0.917	97.0

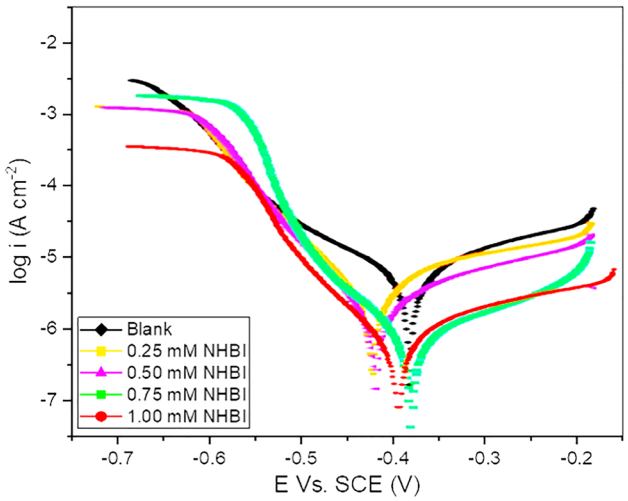

Fig. 5 Polarization curves for X70 steel in 1 M HCl without and in presence of different NBHI concentration at 303 K

$$\eta_{PDP}(\%) = \frac{i^0_{corr} - i'_{corr}}{i^0_{corr}} \times 100 \quad (15)$$

where i^0_{corr} and i'_{corr} are the current densities without and in presence of NBHI, respectively. It is observed from Fig. 3 that the addition of NBHI exerted significant influence on both the cathodic reduction of hydrogen ion $\left(2H^+_{(aq)} + 2e^- \rightarrow H_{2(g)}\right)$ and the anodic X70 steel dissolution ($Fe_{(s)} \rightarrow Fe^{2+}_{(aq)} + 2e^-$). This apparently decreased the current densities of both the cathodic and anodic branches, due to the inhibitor adsorption at the X70 steel surface active sites. The results suggest that NBHI behaves as a mixed-type inhibitor. From Table 5, the i_{corr} values are seen to decrease with increasing concentrations of NBHI, due to increased blockage of greater fraction of the X70 steel surface by adsorption. In addition, it is observed that the E_{corr} values for NBHI in comparison with the blank did not show any obvious trend and with deviation less than 85 mV, confirming that the mixed type behaviour of NBHI (Issaadi et al. 2011; Li et al. 2011).

SEM analysis

SEM images of corroded X70 steel surface which was immersed in 1 M HCl for 7 h without and in presence of inhibitor (Fig. 6a, b) were used to confirm the corrosion inhibitive performance of NBHI for the X70 steel. Proper look at the SEM images indicates that the steel surface without NBHI was more corroded with visible number of pits distributed in the entire metal surface (Fig. 6a). The X70 steel surface in the NBHI inhibited solution looks better with smoother surface, containing fewer pits (Fig. 6b). This observation confirms that NBHI hinders the corrosion of X70 steel by forming adsorbed protective layer on the steel surface.

Quantum chemical analysis

The electronic and structural properties of organic compounds influence their effectiveness as corrosion inhibitors. In the 1 M HCl solution, the studied inhibitor may exist in its protonated form (NBHI-H$^+$) which is in equilibrium with the neutral molecule (NBHI). Based on this, the Frontier molecular orbitals (FMOs) density distributions of both the neutral and protonated NBHI were analysized as depicted in Fig. 7. All computed quantum chemical parameters are displayed in Tables 6. In line with the Fukui's frontier orbital approximation, there is usually an occurrence of donor-acceptor interactions between FMOs (HOMO and LUMO) of reacting/interacting species (Abdallah et al. 2013). There is a high tendency of a metal accepting electron from an inhibitor molecule (an electron donor) into its lowest unoccupied orbital. On the other hand, metals can donate their HOMO electrons to the vacant LUMO orbitals of inhibitor molecules (Murulana et al. 2012; Mashuga et al. 2015) for back-bonding. This relationship of donor-acceptor between metallic orbitals and inhibitor molecules is the basis of electronic and molecular explanation of inhibitor adsorption on metal surfaces. The HOMO of NBHI and NBHI-H$^+$ are mainly localized on the phenol ring, extending along the bromine atom while only that of NBHI-H$^+$ extended to the azomethine group. The LUMO of NBHI are distributed on almost the entire compound apart from the bromine atom

Table 5 Polarization parameters for X70 steel in 1 M HCl without and in presence of different NBHI concentration at 303 K

Concentration (M)	$-E_{corr}$ (mV/SCE)	i_{corr} (μA cm^{-2})	β_a (mV dec^{-1})	$-\beta_c$ (mV dec^{-1})	η_{PDP} (%)
Blank	387	806.7	131.1	101.5	–
0.25	423	292.8	118.4	97.2	63.7
0.50	415	207.3	105.0	81.6	74.3
0.75	382	95.1	96.3	98.5	88.2
1.00	396	46.9	84.6	72.8	94.2

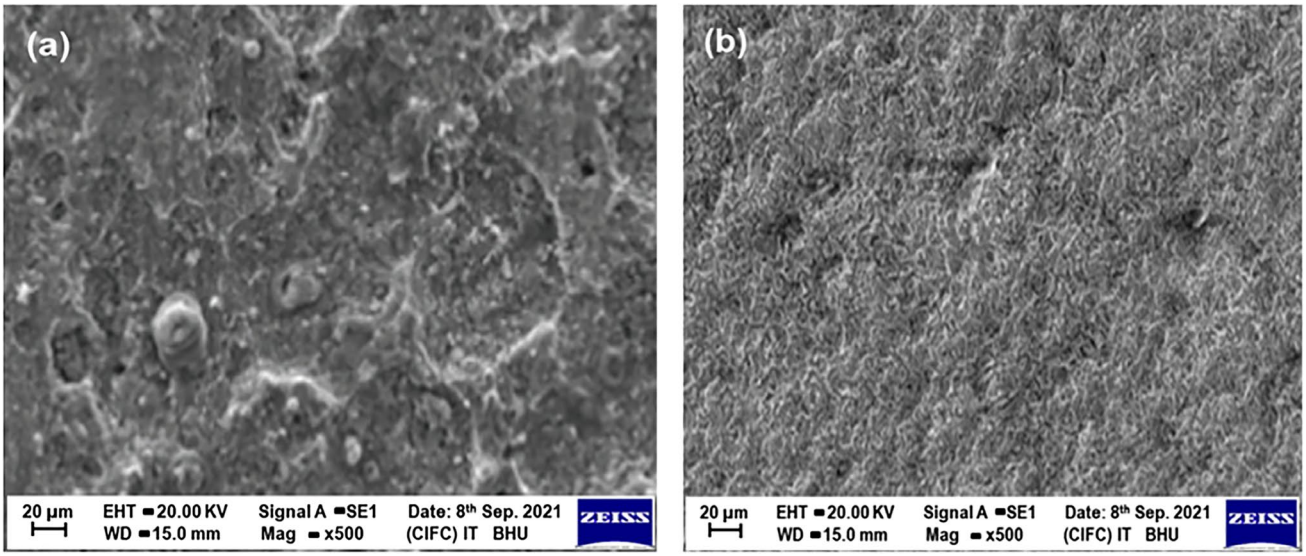

Fig. 6 SEM images of **a** X70 steel in 1 M HCl, **b** X70 steel in 1.00 mM NBHI

while the The LUMO of NBHI-H^+ are mainly distributed on the azine ring. This could be due to the nitrogen heteroatom which is highly electronegative and can make the azine ring relatively electron-deficient.

The computed quantum parameters for NBHI and NBHI-H^+ are listed in Table 6. The E_{HOMO} for NBHI is higher and with lower ΔE whereas the E_{LUMO} for NBHI-H^+ is lower and with higher ΔE. Higher E_{HOMO} is related to higher ability to donate electron and lower E_{LUMO} is in line with higher ability to accept electron. This implies that NBHI-H^+ will accept electrons from metal orbital, while NBHI has a higher capability to donate electron to the surface of the metal. The general inhibitor reactivity is controlled ΔE and it favours NBHI which has a lower ΔE value. NBHI-H^+ indicates lower dipole moment (μ) which favours inhibitor accumulation on the surface of the metal (Khalil 2003). The smaller value of global hardness (η) shows higher contribution of NBHI based on the principle of hard-soft acid base (HSAB) (Herrag et al. 2010).

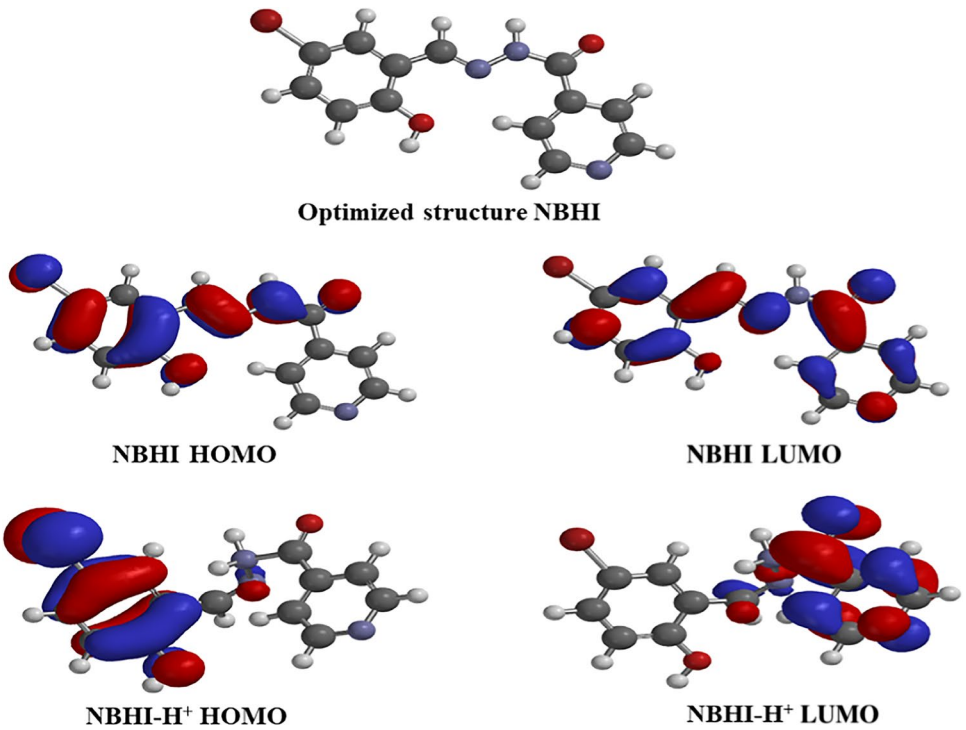

Fig. 7 Optimized structure, HOMO and LUMO for protonated and neutral molecules of NBHI

Table 6 Theoretical parameters for NBHI inhibitor and its protonated (NBHI-H^+) form

Inhibitor	E_{HOMO} (eV)	E_{LUMO} (eV)	ΔE (eV)	χ (eV)	η (eV)	σ (eV^{-1})	ΔN	μ (Debye)
NBHI	−6.20	−1.98	4.22	4.09	2.11	0.47	0.69	4.07
NBHI-H^+	−9.90	−3.43	6.47	6.67	3.24	1.62	0.05	2.35

On the contrary, higher value of global softness (σ) shows that NBHI-H^+ has more reactivity in steel/inhibitor interaction. Generally, the electronegativity (χ) value of NBHI-H^+ is higher than that of NBHI indicating better performance of NBHI-H^+. In addition, $\Delta N < 3.6$ for both NBHI and NBHI-H^+ shows that increasing donation of electron to the steel surface increases the inhibitor efficacy (Lukovits et al. 2001).

Conclusions

Gravimetric, electrochemical impedance spectroscopy tests, potentiodynamic polarization and scanning electron microscopy were used to investigate the performance of a newly synthesized Schiff base, N-(5-bromo-2-hydroxybenzylidene) isonicotinohydrazide (NBHI) as an inhibitor for X70 carbon steel corrosion in 1 M HCl. The inhibition efficiency of the NBHI increased with the increase of NBHI concentration but decreased with rise in temperature. Polarization result reveals that the inhibitor acted as a mixed-type inhibitor. The adsorption of the NBHI inhibitor on X70 steel surface obeyed Langmuir isotherm and the negative ΔG^0_{ads} values show that the adsorption is spontaneous. The SEM images confirm the X70 steel protection from corrosion in 1 M HCl by studied NBHI. The quantum parameters showed that NBHI has the capability to accept/donate electrons from/to appropriate d orbitals of the steel atom and supports the good corrosion performance of the inhibitor.

Data availability All data generated or analysed during this study are included in this published article.

Declarations

Conflict of interest The authors declare no conflict of interest.

References

Abdallah M, Atwa ST, Salem MM, Fouda AS (2013) Synergistic effect of some halide ions on the inhibition of zinc corrosion in hydrochloric acid by tetrahydro carbazole derivatives compounds. Int J Electrochem Sci 8:10001–10021

Abdallah M, Fawzy A, Hawsawi H, Abdel Hameed RS, Al-Juaid SS (2020) Estimation of water-soluble polymers (Poloxamer and pectin) as corrosion inhibitors for carbon steel in acidic medium. Int J Electrochem Sci 15:8129–8144. https://doi.org/10.20964/2020.08.73

Ansari KR, Quraishi MA, Singh A (2014) Schiff's base of pyridyl substituted triazoles as new and effective corrosion inhibitors for mild steel in hydrochloric acid solution. Corros Sci 79:5–15. https://doi.org/10.1016/j.corsci.2013.10.009

Arivazhagan M, Subhasini VP (2012) Quantum chemical studies on structure of 2-amino-5-nitropyrimidine. Spectrochim Acta A 91:402–410. https://doi.org/10.1016/j.saa.2012.02.018

ASTM (2004) Standard practices for laboratory immersion corrosion testing of metals, American society for testing and materials G31-72. International, ASTM

Belfilali I, Chetouani A, Hammouti B, Aouniti A, Louhibi S, Al-Deyab SS (2012) Synthesis and application of 1,7−bis(2-HydroxyBenzamido)-4-Azaheptane and corrosion inhibitor of mild steel in molar hydrochloric acid medium. Int J Electrochem Sci 7:3997–4013

Bentrah H, Rahali Y, Chala A (2014) Gum Arabic as an eco-friendly inhibitor for API, 5L X42 pipeline steel in HCl medium. Corros Sci 82:426–431. https://doi.org/10.1016/j.corsci.2013.12.018

Boumhara K, Bentiss F, Tabyaoui M, Hammouti B (2014) Use of Artemisia Mesatlantica essential oil as green corrosion inhibitor for mild steel in 1 M hydrochloric acid solution. Int J Electrochem Sci 9:1187–1206

Chakravarthy MP, Mohana KN (2013) Inhibition behaviour of some isonicotinic acid hydrazides on the corrosion of mild steel in hydrochloric acid solution. Int J Corros:1–13. https://doi.org/10.1155/2013/854781

Dueke-Eze CU, Fasina TM, Oluwalana AE, Familoni OB, Mphalele JM, Onubuogu C (2020) Synthesis and biological evaluation of copper and cobalt complexes of (5-substituted-salicylidene) isonicotinichydrazide derivatives as antitubercular agents. Sci Afr 9:e00522. https://doi.org/10.1016/j.sciaf.2020.e00522

Ekanem UF, Umoren SA, Udousoro II, Udoh AP (2010) Inhibition of mild steel corrosion in HCl using pineapple leaves- (Ananas Comosus L.) extract. J Mater Sci 45:5558–5566

El Kacimi Y, Touir R, Galai M, Alaoui K, Dkhireche N, Touhami ME (2020) Relationship between silicon, phosphorus content and grain number in mild steels and its corrosion resistance in pickling hydrochloric acid. Int J Ind Chem 11:111–122. https://doi.org/10.1007/s40090-020-00206-0

Farag AA, Hegazy MA (2013) Synergistic inhibition effect of potassium iodide and novel Schiff bases on X65 steel corrosion in 0.5 M H_2SO_4. Corros Sci 74:168–177. https://doi.org/10.1016/j.corsci.2013.04.039

Finšgar M, Jackson J (2014) Application of corrosion inhibitors for steels in acidic media for the oil and gas industry: a review. Corros Sci 86:17–41. https://doi.org/10.1016/j.corsci.2014.04.044

Hegazy MA, Abdallah M, Ahmed H (2010) Novel cationic gemini surfactants as corrosion inhibitors for carbon steel pipelines. Corros Sci 52(9):2897–2904. https://doi.org/10.1016/j.corsci.2010.04.034

Hegazy MA, Hasan AM, Emara MM, Bakr MF, Youssef AH (2012) Evaluating four synthesized Schiff bases as corrosion inhibitors on the carbon steel in 1 M hydrochloric acid. Corros Sci 65:67–76. https://doi.org/10.1016/j.corsci.2012.08.005

Herrag L, Hammouti B, Elkadiri S, Aouniti A, Jama C, Vezin H, Bentiss F (2010) Adsorption properties and inhibition of mild steel corrosion in hydrochloric solution by some newly synthesized diamine derivatives: experimental and theoretical investigations. Corros Sci 52:3042–3051. https://doi.org/10.1016/j.corsci.2010.05.024

Iroha NB, Akaranta O (2020) Experimental and surface morphological study of corrosion inhibition of N80 carbon steel in HCl stimulated acidizing solution using gum exudate from Terminalia Mentaly. SN Appl Sci 2:1514. https://doi.org/10.1007/s42452-020-03296-8

Iroha NB, Dueke-Eze CU (2021) Experimental studies on two isonicotinohydrazide-based Schiff bases as new and efficient inhibitors for pipeline steel erosion corrosion in acidic cleaning solution. Chem Afr 4(3):635–646. https://doi.org/10.1007/s42250-021-00252-w

Iroha NB, Hamilton-Amachree A (2018) Adsorption and anticorrosion performance of Ocimum Canum extract on mild steel in sulphuric acid pickling environment. Am J Mater Sci 8(2):39–44. https://doi.org/10.5923/j.materials.20180802.03

Iroha NB, James AO (2018) Assessment of performance of velvet tamarind-furfural resin as corrosion inhibitor for mild steel in acidic solution. J Chem Soc Nigeria 43(3):510–517

Iroha NB, Nnanna LA (2021) Tranexamic acid as novel corrosion inhibitor for X60 steel in oil well acidizing fluids: surface morphology, gravimetric and electrochemical studies. Prog Color Colorants Coat 14:1–11

Iroha NB, Oguzie EE, Onuoha GN, Onuchukwu AI (2005) Inhibition of mild steel corrosion in acidic solution by derivatives of diphenyl glyoxal, 16th international corrosion congress. Beijing, China

Iroha NB, Akaranta O, James AO (2015) Red onion skin extract-formaldehyde resin as corrosion inhibitor for mild steel in hydrochloric acid solution. Int Res J Pure App Chem 6(4):174–181. https://doi.org/10.9734/IRJPAC/2015/9555

Iroha NB, Madueke NA, Mkpenie V, Ogunyemi BT, Nnanna LB, Singh S, Akpan ED, Ebenso EE (2020) Experimental, adsorption, quantum chemical and molecular dynamics simulation studies on the corrosion inhibition performance of Vincamine on J55 steel in acidic medium. J Mol Struct 129533. https://doi.org/10.1016/j.molstruc.2020.129533

Iroha NB, Dueke-Eze CU, James AO, Fasina TM (2021) Newly synthesized N-(5-nitro-2-hydroxybenzylidene) pyridine-4-amine as a high-potential inhibitor for pipeline steel corrosion in hydrochloric acid medium. Egypt J Pet 30:55–61. https://doi.org/10.1016/j.ejpe.2021.02.003

Issaadi S, Douadi T, Zouaoui A, Chafaa S, Khan MA, Bouet G (2011) Novel thiophene symmetrical Schiff base compounds as corrosion inhibitor for mild steel in acidic media. Corros Sci 53:1484–1488. https://doi.org/10.1016/j.corsci.2011.01.022

James AO, Iroha NB (2019) An investigation on the inhibitory action of modified almond extract on the corrosion of Q235 mild steel in acid environment. IOSR J Appl Chem 12:1–10. https://doi.org/10.9790/5736-1202020110

James AO, Iroha NB (2021) New green inhibitor of Olax subscorpioidea root for J55 carbon steel corrosion in 15% HCl: theoretical, electrochemical, and surface morphological investigation. Emerg Mater. https://doi.org/10.1007/s42247-021-00161-1

Khaled KF, Elhabib OA, El-mghraby A, Ibrahim OB, Ibrahim MAM (2010) Inhibitive effect of thiosemicarbazone derivative on corrosion of mild steel in hydrochloric acid solution. J Mater Environ Sci 1:139–150

Khalil N (2003) Quantum chemical approach of corrosion inhibition. Electrochim Acta 48:2635–2640. https://doi.org/10.1016/S0013-4686(03)00307-4

Lebrini M, Traisnel M, Lagrenee M, Mernari B, Bentiss F (2008) Inhibitive properties, adsorption and a theoretical study of 3,5-bis(n-pyridyl)-4-amino-1,2,4-triazoles as corrosion inhibitors for mild steel in perchloric acid. Corros Sci 50:473–479. https://doi.org/10.1016/j.corsci.2007.05.031

Li X, Deng S, Fu H (2011) Triazolyl blue tetrazolium bromide as a novel corrosion inhibitor for steel in HCl and H_2SO_4 solutions. Corros Sci 53:302–309. https://doi.org/10.1016/j.corsci.2010.09.036

Lukovits I, Kálmán E, Zucchi F (2001) Corrosion inhibitors-correlation between electronic structure and efficiency. Corrosion 57:3–8

Madkour LH, Elroby SK (2015) Inhibitive properties, thermodynamic, kinetics and quantum chemical calculations of polydentate Schiff base compounds as corrosion inhibitors for iron in acidic and alkaline media. Int J Ind Chem 6(3):165–184. https://doi.org/10.1007/s40090-015-0039-7

Madueke NA, Iroha NB (2018) Protecting Aluminium alloy of type AA8011 from acid corrosion using extract from Allamanda cathartica leaves. Int J Innov Res Sci Eng Technol 7:10251–10258. https://doi.org/10.15680/IJIRSET.2018.0710014

Maduelosi NJ, Iroha NB (2021) Insight into the adsorption and inhibitive effect of spironolactone drug on C38 carbon steel corrosion in hydrochloric acid environment. Journal of Bio- and Tribo-Corrosion 7:6. https://doi.org/10.1007/s40735-020-00441-z

Mashuga ME, Olasunkanmi LO, Adekunle AS, Yesudass S, Kabanda MM, Ebenso EE (2015) Adsorption, thermodynamic and quantum chemical studies of 1-hexyl-3-methylimidazolium based ionic liquids as doi: corrosion inhibitors for mild steel in HCl. Materials 8:3607–3632. https://doi.org/10.3390/ma8063607

Messali M, Lgaz H, Dassanayake R, Salghi R, Jodeh S, Abidi N, Hamed O (2017) Guar gum as efficient non-toxic inhibitor of carbon steel corrosion in phosphoric acid medium: electrochemical, Surface, DFT and MD Simulations Studies. J Mol Struct 1145:43–54. https://doi.org/10.1016/j.molstruc.2017.05.081

Mohan P, Usha R, Kalaignan GP, Muralidharan VS (2013) Inhibition effect of benzo hydrazide derivatives on corrosion behaviour of mild steel in 1 M HCl. J Chem:1–7

Murulana LC, Singh AK, Shukla SK, Kabanda MM, Ebenso EE (2012) Experimental and quantum chemical studies of some bis (trifluoromethyl-sulfonyl) imide imidazolium-based ionic liquids as corrosion inhibitors for mild steel in hydrochloric acid solution. Ind Eng Chem Res 51:13282–13299. https://doi.org/10.1021/ie300977d

Narang R, Narasimhan B, Sharma S (2012) A review on biological activities and chemical synthesis of hydrazide derivatives. Curr Med Chem 19:569–612. https://doi.org/10.2174/092986712798918789

Noor EA, Al-Moubaraki AH (2008) Thermodynamic study of metal corrosion and inhibitor adsorption processes in mild steel/1-methyl-4-styryl pyridinium iodides/hydrochloric acid systems. Mater Chem Phys 110:145–154. https://doi.org/10.1016/j.matchemphys.2008.01.028

Okey NC, Obasi NL, Ejikeme PM, Ndinteh DT, Ramasami P, Sherif EM, Akpan ED, Ebenso EE (2020) Evaluation of some amino benzoic acid and 4-aminoantipyrine derived Schiff bases as corrosion inhibitors for mild steel in acidic medium: synthesis, experimental and computational studies. J Mol Liq 315:113773. https://doi.org/10.1016/j.molliq.2020.113773

Ramaganthan B, Gopiraman M, Olasunkanmi LO, Kabanda MM, Yesudass S, Bahadur I, Adekunle AS, Obot IB, Ebenso EE (2015) Synthesized photo-cross-linking chalcones as novel corrosion inhibitors for mild steel in acidic medium: experimental, quantum chemical and Monte Carlo simulation studies. RSC Adv 5:76675–76688. https://doi.org/10.1039/C5RA12097G

Sainia M, Kumar P, Kumar M, Kalavathy R, Mani V, Mishra RK, Majeed ABA, Narasimhana B (2014) Synthesis, in vitro antimicrobial, anticancer evaluation and QSAR studies of N'-(substituted)-4-(butan-2-lideneamino)benzo hydrazides. Arab J Chem 7:448–460. https://doi.org/10.1016/j.arabjc.2013.05.010

Singh A, Lin Y, Obot IB, Ebenso EE, Ansari KR, Quraishi MA (2015) Corrosion mitigation of J55 steel in 3.5% NaCl solution by a macrocyclic inhibitor. Appl Surf Sci 356:341–347. https://doi.org/10.1016/j.apsusc.2015.08.094

Umoren SA (2016) Biomaterials for corrosion protection: evaluation of mustard seed extract as eco-friendly corrosion inhibitor for X60 steel in acid media. J Adhesion Sci Technol 30:1858–1879. https://doi.org/10.1080/01694243.2016.1168339

Yadav M, Kumar S, Sinha RR, Behera D (2013) Experimental and quantum chemical studies on corrosion inhibition performance of Benzimidazole derivatives for mild steel in HCl. Ind Eng Chem Res 52:6318–6328. https://doi.org/10.1021/ie400099q

Zeino A, Abdulazeez I, Khaled M, Jawich MW, Obot IB (2018) Mechanistic study of polyaspartic acid (PASP) as eco-friendly corrosion inhibitor on mild steel in 3% NaCl aerated solution. J Mol Liq 250:50–62. https://doi.org/10.1016/j.molliq.2017.11.160